ChemComm

COMMUNICATION

View Article Online
View Journal | View Issue

Cite this: *Chem. Commun.*, 2021, **57**, 1022

Received 5th November 2020,
Accepted 22nd December 2020

DOI: 10.1039/d0cc07316d

rsc.li/chemcomm

Pillared cobalt metal–organic frameworks act as chromatic polarizers†

Adrian Gonzalez-Nelson, [ab] Chaitanya Joglekar [a] and Monique A. van der Veen *[a]

The ease with which molecular building blocks can be ordered in metal–organic frameworks is an invaluable asset for many potential applications. In this work, we exploit this inherent order to produce chromatic polarizers based on visible-light linear dichroism *via* cobalt paddlewheel chromophores.

Linear dichroism can be defined as the anisotropic absorption of light by a material.[1] This phenomenon is observed in materials that, due to their crystalline or partially ordered structure, show an overall alignment of the transition dipole moments or of nanostructured features on substrates.[2–4] This results in different degrees of light absorption depending on the relative orientation of the polarization direction of light.[2] For this reason, linear dichroic spectroscopy is often used to determine the structural orientation of molecules in matter.[5–9]

In terms of application, the main interest for dichroic materials is their potential use in polarization-sensitive light detectors[2,3,10] and optical components (*e.g.*, polarizers, filters, and waveplates).[11] The search for new dichroic materials is ongoing, arguably dominated by 2D inorganic materials,[3,10–13] which offer the advantage of strong light–matter interactions.[14,15] However, this family of materials entails shortcomings in processing and obtaining high-quality crystals.[3] Among alternatives proposed to overcome these challenges are hybrid perovskites[3,16] and organic molecular crystals.[17,18] While the dichroism of the former type relies on the strongly anisotropic crystal structure (*i.e.*, stacked 2D layers),[19] the latter approach focuses on engineering molecular interactions to achieve a precise alignment of chromophores within the crystal structure. So far, most materials that show intrinsic dichroism are monochromatic, that is, an increase or decrease of the intensity of a single absorption mode simply results in the apparent change of the color's saturation. In contrast, photonic metamaterials, whose properties follow from their nanostructured features,[20] are capable of showing a dichromatic linear dichroism, where changing the polarization of incident light the material leads to two distinct material colors.[21–24] This is a key advantage towards their application in polarimetry spectroscopy, security tags, and hyperspectral imaging, among others.[20,22,24]

Interestingly, with regard to dichroic molecular crystals, the reticular chemistry concept behind metal–organic frameworks (MOFs) may offer a further degree of control over the orientation of molecules while simultaneously facilitating the use of well-known coordination complexes as chromophores. MOFs are based on highly directional coordination bonding, and thorough research in the past two decades has provided an immense library of node and linker geometries which can be rationally selected to achieve desired properties.[25,26] Although the dichroic effect due to guest molecule alignment inside MOF pores has been reported,[27] to the best of our knowledge inherent linear dichroism has surprisingly not been studied in this type of materials.

Here, we show how well-defined MOF structures may be used as platforms that offer more control over the orientation of chromophores in the crystal structure. We show that dichromatic dichroism can be achieved, for the first time as an *intrinsic* materials' property, which provides the potential for easier large scale processing when compared to metamaterials.

By selecting the tetragonal DMOF architecture, $[M_2(1,4\text{-bdc})_2(\text{dabco})]$ (1,4-bdc = 1,4-benzene dicarboxylate, dabco = 1,4-diazabicyclo[2.2.2]octane, and M = Cu^{2+},[28] Zn^{2+},[29] and Co^{2+},[30,31] among others), where 2D sheets of divalent transition metal carboxylate paddlewheels are stacked *via* dabco ligands functioning as pillars (Fig. 1), a complete anisotropic alignment of the metal paddlewheels is achieved. We chose Co^{2+} as metal due to its attractive chromophoric properties, which have already been demonstrated in other MOFs,[32,33] and show how a dichromatic dichroic effect can be obtained for a relatively simple structure.

We obtained large single crystals of $[Co_2(1,4\text{-bdc})_2(\text{dabco})]$ (**1**) in the range of 500 μm long and 50 μm wide by modifying a

[a] *Department of Chemical Engineering, Delft University of Technology, The Netherlands. E-mail: m.a.vanderveen@tudelft.nl*
[b] *DPI, P. O. Box 92, 5600 AX Eindhoven, The Netherlands*

† Electronic supplementary information (ESI) available. See DOI: 10.1039/d0cc07316d

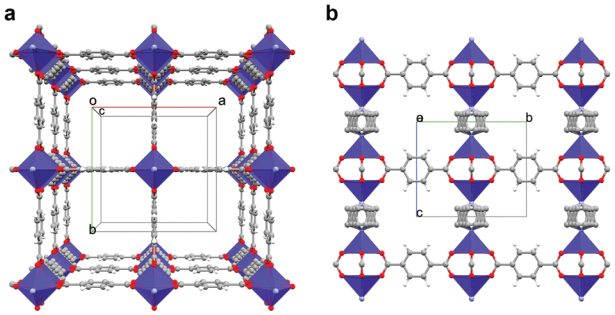

Fig. 1 Structure of **1**. (a) View along [001] direction, *i.e.*, the pillaring axis. (b) View along [100] direction.

previously reported synthesis.[30] pH modulation is a known approach to improve the crystallinity of MOFs.[34,35] During synthesis, protons in solution slow down the kinetics of ligand coordination reactions, thus decreasing nucleation and crystal growth rates. We employed pH modulation by first mixing equimolar amounts of dabco and nitric acid, in order to obtain a monoprotonated dabco-H^+ salt, which was then allowed to react with terephthalic acid and $Co(NO_3)_2{\cdot}H_2O$ in DMF (see ESI† for experimental details). The powder XRD pattern of the product is shown in Fig. S1 (ESI†), alongside the pattern computed from the reported crystallographic structure.

When observed under polarized light, crystals of **1** transmit various colors (blue, purple, orange, yellow, see Fig. 2) depending on their relative orientation to the polarization plane of light. The blue color corresponds to an orientation of the plane of polarization parallel (0°) to the long axis of the crystal, and the yellow color is observed when the crystals are perpendicular to the polarization plane (90°). Intermediate angles result in the combination of both colors. Compared to organic crystals, where dichroism simply manifests as a change in degree of transparence, this change between different colors, is an extraordinary case of dichroism.

To understand the origins of this remarkable dichroism, we first studied the visible light absorption of the MOF. Using diffuse reflectance UV-visible absorption spectroscopy on powdered

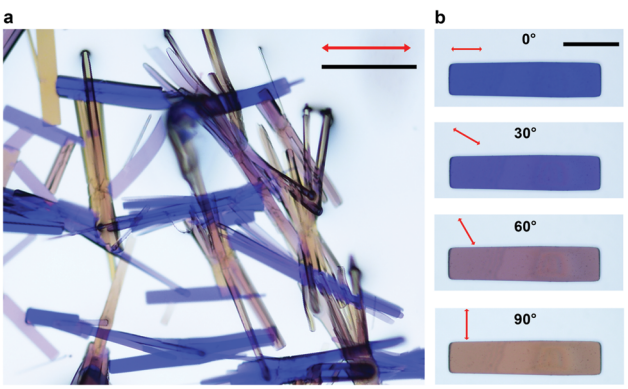

Fig. 2 Optical images of **1**. (a) Various relative orientations with respect to the polarization direction transmit different ranges of visible light. (b) View of an isolated crystal of **1** whose long axis is 0°, 30°, 60°, and 90° relative to the polarized light's orientation (red arrows); scale bars are 200 μm.

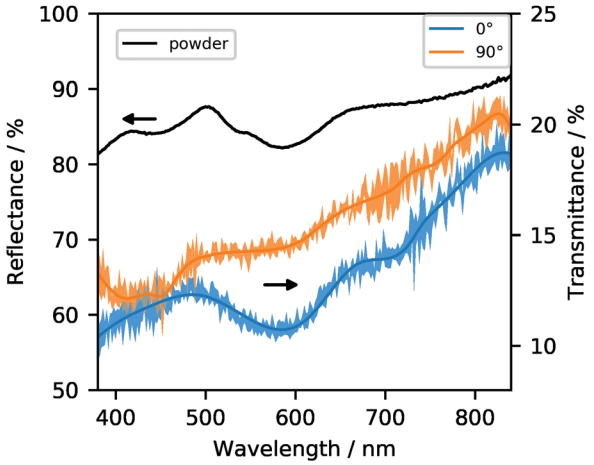

Fig. 3 UV-visible spectra of **1** as powder in diffuse reflectance mode (black) and in single-crystal transmission mode with two relative polarization directions (0° shown in blue and 90° in orange).‡ The shaded area corresponds to one standard deviation (see ESI† for details).

samples, we identified absorption bands at 450, 540, 580, and a very broad absorption band in the range 700–800 nm (Fig. 3). These absorption bands correspond to electronic transitions that are not present in the uncoordinated organic linkers, which do not absorb visible light. Rather, they are related to d–d transitions of electrons in the Co-dimers.[36,37] In fact, the absorption bands are very close to those reported for similar Co-paddlewheel MOFs,[32,38–40] as well as for cobalt complexes with a comparable coordination environment.[41–43]

The tetragonal crystal structure of the framework suggests that the distinct axis (*i.e.*, *c*) corresponds to the long dimension of their square prism habit. This means that the long axis of each crystal corresponds to the [Co–dabco–Co] direction.

Polarization-dependent UV-visible absorbance spectroscopy on single crystals in transmission allows to understand how the different absorption bands are involved in the dichroic effect. The single-crystal spectra in Fig. 3 resemble the powder spectrum. However, the difference between the spectrum at 0° and 90° shows a clear change governing the transition from blue to yellow in the relative strength of the absorption bands centered around 580 and, to a lesser degree, 720 nm. The latter may indicate that the broad absorption observed in the powder spectrum is in fact several partially overlapping transitions in the 700–800 nm range. At 0°, the 580 nm absorption is at its maximum, meaning that a larger fraction of yellow light is absorbed, causing the crystal to appear blue.[44] At 90°, absorption of the 580 band is drastically decreased, implying that this wavelength's transmittance through the crystal increases, which results in it dominating the optical appearance. The weaker absorption at *ca.* 720 nm undergoes a similar decrease, although it is less noticeable given the confidence intervals. An apparent inverse effect where absorption becomes stronger at 90° may be inferred from the 450 nm absorption band (corresponding to the absorption of blue light), but the limited signal-to-noise ratio of these experiments does not allow us to conclude this with certainty. Also note that the yellow color of the crystals under

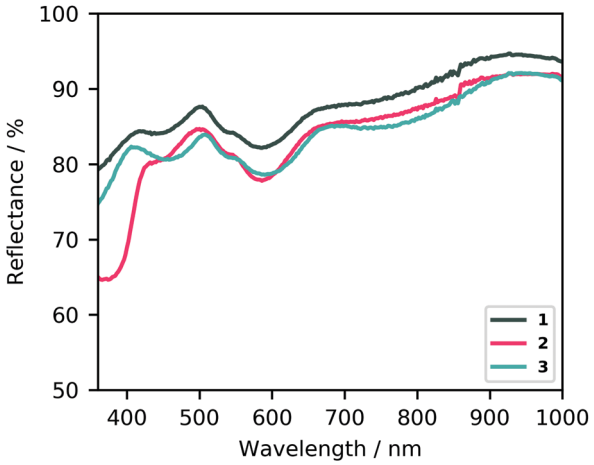

Fig. 4 Diffuse reflectance UV-visible spectra of **1**, **2**, and **3**. Barring the absorption at 375 nm for **2**, the same absorption bands are observed for all frameworks, with slight shifts with respect to **1**.

90° implies significant absorption of blue light (the 450 nm band), in contrast to the blue crystals at 0° where blue light is the least absorbed.

These observations can be rationalized by considering the framework's crystal structure. Within the pillared structure, the cobalt dimers are aligned along the *c* axis, which corresponds to the longest dimension of the crystal habit. Therefore, in combination with the UV-visible absorption evidence, we can propose that the transition dipole moment corresponding to the 580 nm centered transition, as well as the 720 nm transition, are located along this axis. The higher energy absorption around 450 nm remains present at 90° polarization angle, causing the crystal to appear yellow.[45] This particular transition between two modes of visible light absorption is uncommon in dichroic materials, which are often monochromatic.[17,18,27,46]

The dichromatic dichroic effect is retained upon functionalization of the BDC linkers with nitro and amino groups (compounds $[Co_2(1,4\text{-bdc-}NH_2)_2(dabco)]$ (**2**) and $[Co_2(1,4\text{-bdc-}NO_2)_2(dabco)]$ (**3**); synthesis and characterization in ESI†). Only slight shifts in the location of absorption bands are observed (Fig. 4), as well as the appearance of a new absorption band in the case of the amino functionalization (at *ca.* 375 nm), assigned to an n–π* transition in previous work with the same linker.[47] The visible light dichroic effect in these two MOFs is very similar to that of the unfunctionalized framework, with the largest difference between 0° and 90° polarization being the absorption at 580 and 720 nm (the latter to a lesser degree), producing a change from blue to yellow appearance under the optical microscope, respectively (Fig. S2 and S3, ESI†). This is not unexpected, because the coordination geometry of the Co-paddlewheel chromophore likely remains unchanged, and the electronic effects of the benzene ring substituent only have an indirect impact on the energy levels of the d–d transitions responsible for the dichroic absorption of visible light. The linkers, however, do provide a handle for additional dichroism in the near UV-range.

Since the observed dichroism is a result of d–d transitions from the cobalt coordination environment, the substitution of this metal should lead to a modification of the effect. This pillared structure thus provides an excellent playground to tune the dichroism to different combinations of colors. Potential pathways for such tunability would include the substitution of the metal cations (*e.g.*, with Cu^{2+} or Mn^{2+}), or of the pillaring linker with a different nitrogen donor ligand, which can be expected to modify the splitting of the visible-light transitions significantly.

The ordered structure and specific orientation of building blocks are exceptional features with a tunable character in MOFs, which enable the development of new materials with desirable light-matter interactions. In the case of Co-based DMOFs, an anisotropic family of pillared frameworks, we show how an unprecedented visible-light dichroic behavior that is dichromatic. So far, to the best of our knowledge, such properties have only been achieved by applying nanostructured metamaterials as chromatic plasmonic polarizes.[24] MOFs may therefore be an attractive alternative to the complex nanopatterning processes currently needed for plasmonic polarizers.[20] The results presented here would be the first example of dichromatic dichroism being an intrinsic material property. We propose that this strategy can be used to produce versatile dichroic materials active in other ranges of the electromagnetic spectrum, provided that the linker (or linkers), the inorganic building units, and therefore the topology, are selected accordingly.

The work of A. G.-N. forms part of the research program of DPI, NEWPOL project 731.015.506. M. A. v. d. V. is grateful for funding by the European Research Council (grant number 759212) within the Horizon 2020 Framework Programme (H2020-EU.1.1).

Conflicts of interest

There are no conflicts to declare.

Notes and references

‡ Although the reported transmittance seems low, it is important to remark that reflectance on the crystal surfaces may play a role in addition to absorbance, as the reference in the UV-Vis spectroscopy measurements entailed a cell without a crystal present. Nevertheless, the reflectance is expected to be similar in both polarization orientations, meaning that the relative change between the two single-crystal spectra is due to the dichroic effect.

1 B. Nordén, *Appl. Spectrosc. Rev.*, 1978, **14**, 157–248.
2 H. Yuan, X. Liu, F. Afshinmanesh, W. Li, G. Xu, J. Sun, B. Lian, A. G. Curto, G. Ye, Y. Hikita, Z. Shen, S. C. Zhang, X. Chen, M. Brongersma, H. Y. Hwang and Y. Cui, *Nat. Nanotechnol.*, 2015, **10**, 707–713.
3 Y. Liu, Z. Wu, X. Liu, S. Han, Y. Li, T. Yang, Y. Ma, M. Hong, J. Luo and Z. Sun, *Adv. Opt. Mater.*, 2019, **7**, 2–7.
4 Y. Liu, J. Wang, S. Han, X. Liu, M. Li, Z. Xu, W. Guo, M. Hong, J. Luo and Z. Sun, *Chem. – Eur. J.*, 2020, **26**, 3494–3498.
5 S. Rocha, M. Kogan, T. Beke-Somfai and B. Nordén, *Langmuir*, 2016, **32**, 2841–2846.
6 M. R. Hicks, J. Kowalski and A. Rodger, *Chem. Soc. Rev.*, 2010, **39**, 3380–3393.
7 T. Biver, *Appl. Spectrosc. Rev.*, 2012, **47**, 272–325.
8 N. E. Persson, S. Engmann, L. J. Richter and D. M. DeLongchamp, *Chem. Mater.*, 2019, **31**, 4133–4147.

9 J. Qiao, X. Kong, Z.-X. Hu, F. Yang and W. Ji, *Nat. Commun.*, 2014, **5**, 4475.
10 Z. Zhou, M. Long, L. Pan, X. Wang, M. Zhong, M. Blei, J. Wang, J. Fang, S. Tongay, W. Hu, J. Li and Z. Wei, *ACS Nano*, 2018, **12**, 12416–12423.
11 J. Yu, X. Kuang, Y. Gao, Y. Wang, K. Chen, Z. Ding, J. Liu, C. Cong, J. He, Z. Liu and Y. Liu, *Nano Lett.*, 2020, **20**, 1172–1182.
12 X. Wang, Y. Li, L. Huang, X.-W. Jiang, L. Jiang, H. Dong, Z. Wei, J. Li and W. Hu, *J. Am. Chem. Soc.*, 2017, **139**, 14976–14982.
13 S. Yang, C. Hu, M. Wu, W. Shen, S. Tongay, K. Wu, B. Wei, Z. Sun, C. Jiang, L. Huang and Z. Wang, *ACS Nano*, 2018, **12**, 8798–8807.
14 M. Long, P. Wang, H. Fang and W. Hu, *Adv. Funct. Mater.*, 2019, **29**, 1803807.
15 F. H. L. Koppens, T. Mueller, P. Avouris, A. C. Ferrari, M. S. Vitiello and M. Polini, *Nat. Nanotechnol.*, 2014, **9**, 780–793.
16 Y.-Q. Zhao, Q.-R. Ma, B. Liu, Z.-L. Yu, J. Yang and M.-Q. Cai, *Nanoscale*, 2018, **10**, 8677–8688.
17 J.-C. Christopherson, K. P. Potts, O. S. Bushuyev, F. Topić, I. Huskić, K. Rissanen, C. J. Barrett and T. Friščić, *Faraday Discuss.*, 2017, **203**, 441–457.
18 O. S. Bushuyev, T. Friščić and C. J. Barrett, *Cryst. Growth Des.*, 2016, **16**, 541–545.
19 L. Li, X. Liu, Y. Li, Z. Xu, Z. Wu, S. Han, K. Tao, M. Hong, J. Luo and Z. Sun, *J. Am. Chem. Soc.*, 2019, **141**, 2623–2629.
20 H. Jia, Q. J. Wu, C. Jiang, H. Wang, L. Q. Wang, J. Z. Jiang and D. X. Zhang, *Appl. Opt.*, 2019, **58**, 704.
21 Y. Jung, H. Jung, H. Choi and H. Lee, *Nano Lett.*, 2020, **20**, 6344–6350.
22 Z. Li, A. W. Clark and J. M. Cooper, *ACS Nano*, 2016, **10**, 492–498.
23 D. Franklin, R. Frank, S.-T. Wu and D. Chanda, *Nat. Commun.*, 2017, **8**, 15209.
24 T. Ellenbogen, K. Seo and K. B. Crozier, *Nano Lett.*, 2012, **12**, 1026–1031.
25 O. M. Yaghi, *ACS Cent. Sci.*, 2019, **5**, 1295–1300.
26 O. M. Yaghi, M. O'Keeffe, N. W. Ockwig, H. K. Chae, M. Eddaoudi and J. Kim, *Nature*, 2003, **423**, 705–714.
27 I. M. Walton, J. M. Cox, J. A. Coppin, C. M. Linderman, D. G. (Dan) Patel and J. B. Benedict, *Chem. Commun.*, 2013, **49**, 8012.
28 K. Seki, S. Takamizawa and W. Mori, *Chem. Lett.*, 2001, 332–333.
29 D. N. Dybtsev, H. Chun and K. Kim, *Angew. Chem., Int. Ed.*, 2004, **43**, 5033–5036.
30 H. Wang, J. Getzschmann, I. Senkovska and S. Kaskel, *Microporous Mesoporous Mater.*, 2008, **116**, 653–657.
31 T. Takei, T. Ii, J. Kawashima, T. Ohmura, M. Ichikawa, M. Hosoe, Y. Shinya, I. Kanoya and W. Mori, *Chem. Lett.*, 2007, **36**, 1136–1137.
32 S. Ehrling, I. Senkovska, V. Bon, J. D. Evans, P. Petkov, Y. Krupskaya, V. Kataev, T. Wulf, A. Krylov, A. Vtyurin, S. Krylova, S. Adichtchev, E. Slyusareva, M. S. Weiss, B. Büchner, T. Heine and S. Kaskel, *J. Mater. Chem. A*, 2019, **7**, 21459–21475.
33 M. Andrzejewski and A. Katrusiak, *J. Phys. Chem. Lett.*, 2017, **8**, 279–284.
34 S. Canossa, A. Gonzalez-Nelson, L. Shupletsov, M. del Carmen Martin and M. A. Van der Veen, *Chem. – Eur. J.*, 2020, **26**, 3564–3570.
35 Y. Zhao, Q. Zhang, Y. Li, R. Zhang and G. Lu, *ACS Appl. Mater. Interfaces*, 2017, **9**, 15079–15085.
36 N. Benbellat, K. S. Gavrilenko, Y. Le Gal, O. Cador, S. Golhen, A. Gouasmia, J. M. Fabre and L. Ouahab, *Inorg. Chem.*, 2006, **45**, 10440–10442.
37 *Conducting and Magnetic Organometallic Molecular Materials*, ed. M. Fourmigué and L. Ouahab, Springer Berlin Heidelberg, Berlin, Heidelberg, 2009, vol. 27.
38 J. Zhu, J. Chen, T. Qiu, M. Deng, Q. Zheng, Z. Chen, Y. Ling and Y. Zhou, *Dalton Trans.*, 2019, **48**, 7100–7104.
39 V. Gupta and S. K. Mandal, *Dalton Trans.*, 2019, **48**, 415–425.
40 X. Yang, Y. Zhang, F. Li, T. Guo, Y. Wu, F. Jin, M. Fang, Y. Lan, Y. Li, Y. Zhou and Z. Zou, *Dalton Trans.*, 2017, **46**, 8204–8218.
41 J. Hudák, R. Boča, Ľ. Dlháň, J. Kožíšek and J. Moncoľ, *Polyhedron*, 2011, **30**, 1367–1373.
42 J. Catterick and P. Thornton, *J. Chem. Soc., Dalton Trans.*, 1976, 1634.
43 M. Ciampolini and I. Bertini, *J. Chem. Soc. A*, 1968, 2241.
44 J. Cenens and R. A. Schoonheydt, *Clays Clay Miner.*, 1988, **36**, 214–224.
45 M. Šuleková, A. Hudák and M. Smŕcová, *Molecules*, 2016, **21**, 1368.
46 I. M. Walton, J. M. Cox, T. B. Mitchell, N. P. Bizier and J. B. Benedict, *CrystEngComm*, 2016, **18**, 7972–7977.
47 D. Sun, Y. Fu, W. Liu, L. Ye, D. Wang, L. Yang, X. Fu and Z. Li, *Chem. – Eur. J.*, 2013, **19**, 14279–14285.